InP quantum dots: Electronic structure, surface effects, and the redshifted emission

Huaxiang Fu and Alex Zunger
National Renewable Energy Laboratory, Golden, Colorado 80401
~Received 16 December 1996!

We present pseudopotential plane-wave electronic-structure calculations on InP quantum dots in an effort to understand quantum confinement and surface effects and to identify the origin of the long-lived and redshifted luminescence. We find that ~i! unlike the case in small GaAs dots, the lowest unoccupied state of InP dots is the Γ_{1c}-derived direct state rather than the X_{1c}-derived indirect state and ~ii! unlike the prediction of $\mathbf{k}\cdot\mathbf{p}$ models, the highest occupied state in InP dots has a $1sd$-type envelope function rather than a ~dipole-forbidden! $1pf$ envelope function. Thus explanations ~i! and ~ii! to the long-lived redshifted emission in terms of an orbitally forbidden character can be excluded. Furthermore, ~iii! fully passivated InP dots have no surface states in the gap. However, ~iv! removal of the anion-site passivation leads to a P dangling bond ~DB! state just above the valence band, which will act as a trap for photogenerated holes. Similarly, ~v! removal of the cation-site passivation leads to an In dangling-bond state below the conduction band. While the energy of the In DB state depends only weakly on quantum size, its radiative lifetime increases with quantum size. The calculated ; 300-meV redshift and the ; 18 times longer radiative lifetime relative to the dot-interior transition for the 26-Å dot with an In DB are in good agreement with the observations of full-luminescence experiments for unetched InP dots. Yet, ~vi! this type of redshift due to surface defect is inconsistent with that measured in *selective* excitation for HF-etched InP dots. ~vii! The latter type of ~''resonant''! redshift is compatible with the calculated *screened* singlet-triplet splitting in InP dots, suggesting that the slow emitting state seen in selective excitation could be a triplet state. @S0163-1829~97!04428-7#

I. INTRODUCTION

One of the interesting features of the spectroscopy of quantum dots is the almost universal occurrence of a redshift of the emission relative to the absorption. This was seen in quantum dots of Si,[1–6] CdSe,[7–15] InP,[16,17] and InGaAs ~Refs. 18 and 19! and exists irrespectively of the preparation methods of the dots, whether it is based on colloidal chemistry[7–17] or on strain-induced dot formation.[18,19] One obvious reason for the redshift is the existence of a residual size distribution even in the best prepared dot samples: The larger dots in a sample have lower band-edge energies @horizontal lines in Fig. 1~a!#, so if one excites a sample with sufficiently-high-energy photons above the band edge of the smallest dot @a ''global excitation'' experiment; see Fig. 1~c!#, the emission will be redshifted because it results from the deexcitation of band edges of *all* the dots in the sample. The corresponding size-dependent ''nonresonant Stokes shift'' Δ_{nonres}, the difference between the lowest-energy peak in the absorption spectra and the emission peak @see Fig. 1~c!#, is large @ ; 100 meV in CdSe ~Ref. 13! and ; 200 meV for InP ~Refs. 16 and 17!#. It is possible, however, to eliminate much of the effect of size distribution by exciting selectively only the largest dots in a sample, using sufficiently-low-energy photons. Such a ''selective excitation'' experiment @also

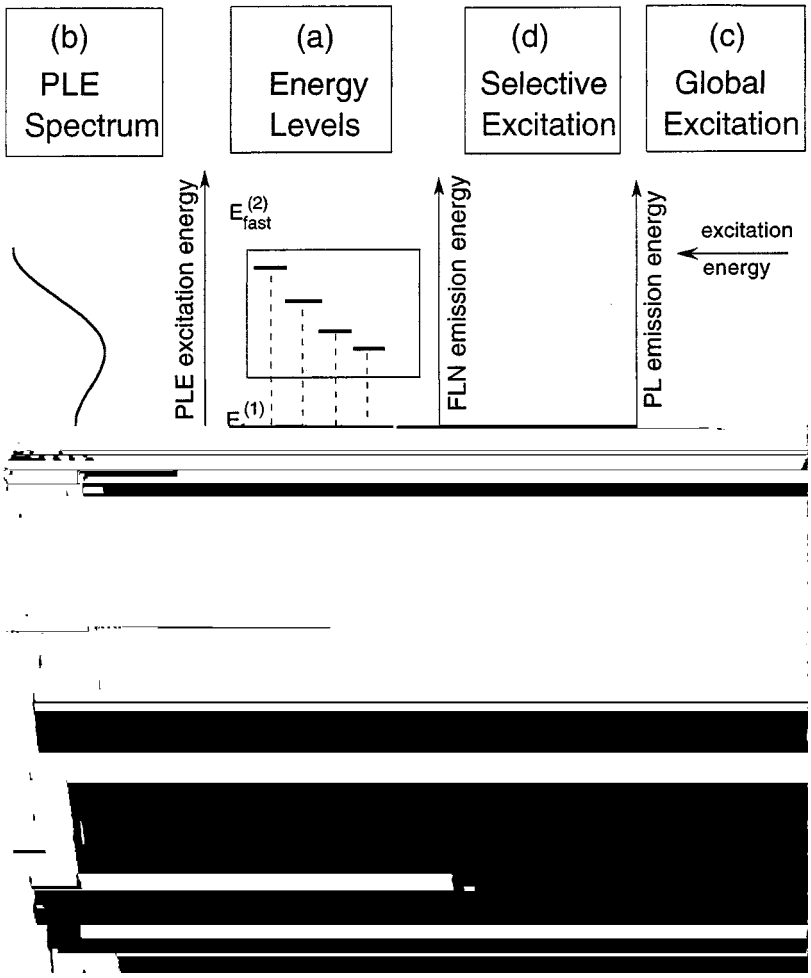

FIG. 1. Schematic diagram illustrating how the basic spectroscopic information in quantum dots is obtained via absorption and emission experiments. ~a! The excited energy levels of the dots present in a given sample form groups: the lowest-energy group $\{E_{\rm slow}\}$ comprises states that are largely forbidden to the ground state

$-E_{\rm slow}$ energy splitting in selectively excited photoluminescence ~PL!. However, Takagahara[20] criticized the work of Martin *et al.*,[23] showing that a more accurate description of dielectric screening, using the screening constant $\epsilon_x \simeq 3$, produces an exchange splitting in agreement with experiment. A recent calculation[24] of exchange splitting from accurate *microscopic* wave functions casts doubt, however, on previous estimates[20,23] of the exchange splittings based on envelope-function calculations. A model including exchange splitting was also used recently by Efros *et al.*[13] to explain the spectroscopic results on CdSe dots. In this approach, the four highest ~$1sd$-like! hole states ~i.e., neglecting split-off band! of a spherical dot are allowed to couple with the two lowest ~$1s$-like! electron states to produce eight electron-hole excitonic states. A $\mathbf{k}\cdot\mathbf{p}$ calculation in this subspace, using phenomenological exchange integrals and numerous parameters, shows that the lowest exciton state is spin forbidden ~''dark exciton'' $\{E_{\rm slow}\}$!, while only higher-energy states $\{E_{\rm fast}\}$ are allowed ~''bright exciton''!. Using a number of parameters, this model explained[13] the observed resonant redshift as the splitting between $E_{\rm slow}$ and the lowest $E_{\rm fast}$, while the nonresonant redshift is explained as the splitting between the center of gravity of *all* dipole-allowed states and $E_{\rm slow}$. Recent magnetic-field experiments were consistent with this model.[13] A recent calculation by Richard *et al.*[25] showed, however, that the inclusion of six rather than four valence bands in the $\mathbf{k}\cdot\mathbf{p}$ Hamiltonian can produce in CdSe a symmetry forbidden $1pf$ ~rather than $1sd$! hole state *even without an exchange interaction*. Thus the $\{E_{\rm slow}\}$ to $\{g\}$ transition could be *spatially* forbidden, not spin forbidden.

(ii) Intrinsic, orbitally forbidden conduction state. The lowest-energy electron-hole state $|E_{\mathrm{slow}}\rangle$ could be dipole forbidden to the ground state $|g\rangle$ if the single-particle electron component of $|E_{\mathrm{slow}}\rangle$ is *spatially forbidden* with respect to $|g\rangle$ due to the difference of *Bloch wave functions* for these two states. For example, if the one-electron valence-band maximum ~VBM! is a Γ_{15v}-like state, but the one-electron conduction-band minimum ~CBM! is an X_{1c}-like state, the zero-phonon single-particle $\Gamma_{15v}\rightarrow X_{1c}$ transition dipole will be zero. Of course, multiband intervalley mixing due to the finite size of dot can relax this strict condition somewhat, leading to a finite transition probability ~long radiative lifetime!. In general, an X_{1c}-like CBM in a dot can occur as follows: In zinc-blende semiconductors, the effective mass of Γ electrons is lighter than that of X electrons, so as the nanocrystallite becomes smaller, the conduction band at Γ moves upward ~due to kinetic-energy confinement! at a

for the identity of the slow, redshifted emission in particular dots and model it in detail without comparing it to alternative explanations. For example, Efros *et al.*[13] examined for CdSe the effect ~i! of an intrinsic, spin-forbidden state; Richard *et al.*[25] examined for a few semiconductor dots the effect ~iii! of an intrinsic, orbitally forbidden valence state, while Grigoryan *et al.*[27] examined it for CdS; Garilenko, Vogl, and Koch[42] examined for Si the effect ~iv! of surface states and Tsiper[43] offered a ''universal explanation'' that is independent of any feature of the electronic structure of the dots.

~c! Most theoretical approaches employ the parameters that either lack independent verification ~e.g., the scaled exchange splitting in Ref. 13! or have a significant range of numerical uncertainty ~e.g., the $\mathbf{k}\cdot\mathbf{p}$ parameters in Ref. 25!. In many cases, unfortunately, the conclusions appear to be sensitive to the parameter choices.

In this work, we study the possible origins of the lowest, slow-emitting electronic states in InP quantum dots including the possibilities of surface effect and excitonic exchange splitting. We use a computational approach that includes an explicit dot surface. The electronic structure is calculated both for the fully passivated surface as well as for dot surfaces in which a cation surface dangling bond or an anion surface dangling bond is created. We find the following.

~a! The CBM of an InP dot is *not* derived from the X_{1c} state even for small dots, so model ~ii! can be excluded for InP.

~b! The symmetry of the envelope function of the VBM is $1sd$-like ~unlike what current $\mathbf{k}\cdot\mathbf{p}$ models[25] predict!, so model ~iii! can be excluded also.

~c! Regarding the surface state model @mechanism ~iv!#, we find that *passivated dots have no surface states in the gap*. In fact, we predict that over a wide range of different passivation species the band-edge states of the dots will be unchanged.

~d!

obtained[45] by fitting the surface density states of the *flat*, chemically passivated InP surfaces ~without reconstruction! to the photoluminescence data.[48] Assuming the same atomic density as in the bulk, the effective dot diameters are given by[49] $d=(a/2)N^{1/3}$, where a is the lattice constant of bulk InP ~5.83 Å! and N is number of atoms in the dots. This gives the effective sizes of 13.83, 18.57, 26.01, and 42.87 Å for the above four dots. The numbers of plane-wave basis functions used in calculation are 31 287, 52 519, 102 733, and 315 969, respectively.

Such huge Hamiltonian matrices cannot be solved by ordinary diagonalization methods. We use instead the ''fold spectrum method''[28] in which $Hc=$

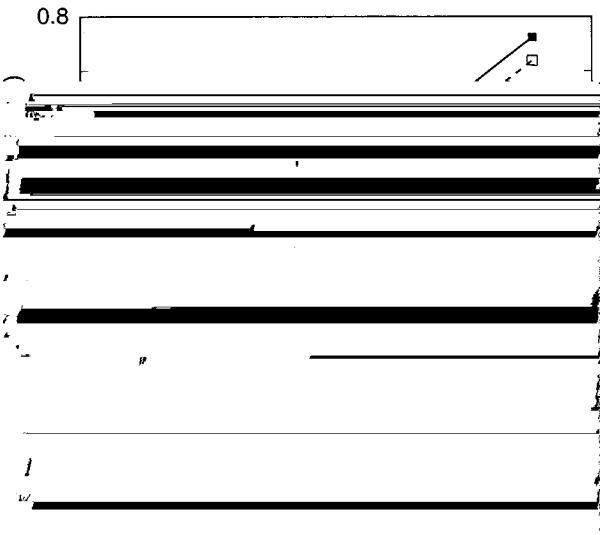

FIG. 5. Calculated resonant redshift in InP quantum dots versus the excitonic gaps, showing ~a! the redshifts due to the surface-state mechanism ~including a single In dangling bond and interacting dangling bonds! and ~b! the redshift due to exchange splittings calculated with the distance-dependent Thomas-Fermi dielectric screening constant. The lines in this figure are a guide for eyes.

where c_e and c_h are, respectively, the electron and hole single-particle wave functions and are obtained from our direct pseudopotential calculation of Eq. ~1!. Here the distance-dependent Thomas-Fermi dielectric function[56] is used to describe the screening of the exchange interaction, i.e.,

$$\varepsilon(r)=\begin{cases}\varepsilon(0,d)\,\dfrac{qR}{\sinh[q(R-r)]+qr}, & r<R\\ \varepsilon(0,d), & r>R\end{cases} \qquad (4)$$

where $q^2=4(3\pi^2 n_0)^{1/3}/\pi$ (n_0 is the average density of the valence electrons at the equilibrium volume) and R is the screening length determined by

$$\sinh(qR)/qR=\varepsilon(0,d). \qquad (5)$$

Note that for large r, the function $\varepsilon(r)$ approaches the value $\varepsilon(0,d)$. The static dielectric constant $\varepsilon(0,d)$ in the quantum dot is different from the bulk value[57] and depends on the dot size d. We use for $\varepsilon(0,d)$ the modified Penn model,[57,58] i.e., $\varepsilon(0,d)=1.0+11.4/[1.0+(12.094/d)^2]$ (the size d is in units of angstroms).

Our calculated exchange splittings for cubic dots with effective diameters of 13.81, 18.57, and 26.01 Å are 52.9, 24.1, and 10.4 meV, respectively. We also calculate the exchange splittings for some spherical dots and obtain the exchange values of 37.9, 22.0, and 8.8 meV for dot sizes 16.02, 23.68, and 34.79 Å, respectively. This shows that the exchange splittings in dots are substantially enhanced compared with the bulk (; 1 meV). The calculated exchange splittings for different dot sizes are plotted in Fig. 5 as a function of the excitonic gap. The relationship is seen to be nearly linear.

The fact that screening the exchange by $\varepsilon(r)$ [Eq. (4)] affects significantly the numerical value of the exchange shows that at large-r values the exchange interactions are not negligible. Thus, contrary to previous assumptions, our calculation supports the view that exchange interactions in dots are not short ranged.

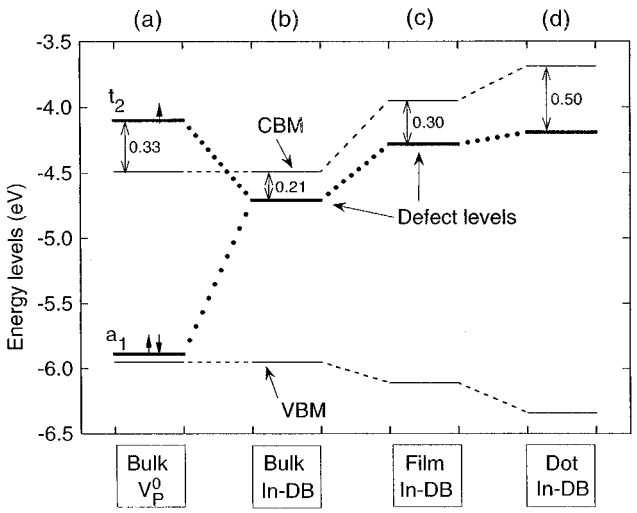

FIG. 6. Energy levels for different In dangling-bond defects: ~a! a neutral P vacancy in bulk InP, giving rise to four In dangling bonds; ~b! a single In dangling bond in bulk; ~c! a single In dangling bond at the 9-ML InP~110! film; and ~d! a single In dangling bond at the surface of the $d=18.57$ Å dot.

C. Electronic structure of dots with model surface dangling bond

Given that fully passivated dots have no surface states, we now remove deliberately passivating atom so as to expose surface dangling bonds. The calculation described in what follows is a model calculation, in that we do not know the actual, potentially complex structure of the real surface of a colloidal dot. Generally, such a surface could include many interacting dangling bonds, ''weak'' surface bonds, partially reconstructed surface patches, and various surface-ligand bonding configurations. Our approach is to first model the surface of the *fully passivated* dots after the experimental results of flat, passivated InP surfaces[48] ~in which reconstruction is removed via chemisorption! and then create an isolated In dangling bond ~DB! and separately an isolated P dangling bond to study their generic effects on the electronic structure of the quantum dot. Such isolated dangling bonds represent, most likely, a stronger perturbation than what would be expected to occur in a real surface, having interacting and partially rebonded dangling bonds.

We position the In and P dangling bonds near the center of the dot surface formed on the ~110! plane. Dangling bonds at other sites were also studied. Due to the highly localized nature of the dangling-bond wave functions, we found only slight difference ~less than 0.15 eV! in the energy levels, depending on the precise position of the dangling bond.

1. The indium dangling bond at the dot surface

Figure 6 shows the relative energy position of an In dangling-bond state in a small dot ($d=18.38$ Å), clarifying how this state evolves from the bulk vacancy states. Creation of a neutral P vacancy (V_P^0) in bulk InP produces four In dangling bonds, giving rise to a doubly occupied singly de-

generate a_1 state near the VBM and a singly occupied triply degenerate t_2 state above the CBM @Fig. 6~a!#.[59–63] The interaction between these four dangling bonds spreads their energies: The energy difference between the a_1 state and the *isolated* DB energy is three times the difference between t_2 state and the isolated DB energy.[64] To create a *single* isolated DB, we then passivate three of the four bulk DB's. The a_1 and t_2 levels of the bulk vacancy then give rise to a single bulk In DB state near the CBM @Fig. 6~

a_1 and t_2 levels give rise to a single DB state just above the VBM @Fig. 9~b!#. This level is nearly constant in energy at the InP~110! film @Fig. 9~c!# and at the surface of dot @Fig. 9~d!#, except that the VBM energies are lowered due to quantum confinement. Analyses of the P DB defect-level wave functions show that they are more localized than the In DB wave functions. Additionally, unlike the sp-hybrid nature of In DB wave functions, the P DB wave functions are pure p-like. Figure 10 shows the planar-averaged wave-function squares of the near-edge states of an $(InP)_{712}$ dot with P DB. The P DB state is highly localized at the dot surface, while the VBM and CBM states are extended in the interior of the dot.

Figure 11 shows the energy dependences of the P DB state, the VBM state, and the CBM state on the dot size. Owing to the extreme localization of its wave function, the energy of the P DB state is almost independent of the dot size. However, as Table III shows, the presence of a P dangling bond shifts the dot VBM upward relative to the VBM of the fully passivated dot @by as much as 250 meV for $(InP)_{107}$#, while the dot CBM does not change much. Table III also shows that the shift of the dot VBM due to the P dangling bond is much larger than the shift of the dot CBM due to the In dangling bond, especially for small dots.

Table II shows the dipole matrix elements of the localized-to-extended P DB to CBM transition, indicating that this is a weak transition with a long radiative lifetime, while the extended-to-extended VBM to CBM transition is much stronger and has a shorter radiative lifetime. The P DB state, being just above the valence band ~see Fig. 11!, can act as a trap to photogenerated holes from the valence band. Thus, if P DB's exist, they will trap holes and lead to long hole lifetimes. In practice, owing to the chemical reactivity of a P DB site, it is likely to have but a small concentration.[16]

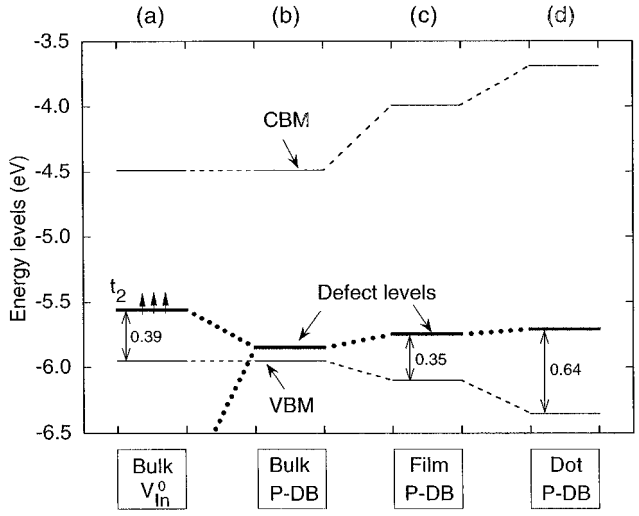

FIG. 9. Energy levels for different P dangling-bond defects: ~a!

D. Discussion of surface dangling bonds and exchange effects

We have seen that our theory excludes two possible mechanisms for the red-shifted, slow emissions in InP dots, namely, $\Vert E_{slow} \&$ cannot be due to ~ii! an intrinsic, orbitally forbidden conduction state or ~iii! an intrinsic, orbitally forbidden valence state. Also, the near-valence-band P DB surface state is not a likely candidate to explain a near-conduction-band shift observed experimentally. We are left

with two possibilities, i.e., the In surface dangling-bond state and the exchange splitting mechanism.

1. Global excitation experiments and the In DB state

Our theoretical results on the In DB surface defect can be compared with experimental *global excitation measurements*,[16] in which different chemical etchants and passivants @tri-*n*-octylphosphine oxide ~TOPO! and HF# were used to etch and passivate the InP quantum dots. Two types of global PL peaks were observed: a short lifetime ~5–50 nsec at $T=300$ K! peak, which does not change its energy for different surface passivants, suggesting that it originates from an intrinsic, dot-interior state; and a long-lifetime ~500 nsec at $T=300$ K! PL peak, which dramatically reduces its intensity when the dot is passivated by HF, suggesting that it could originate from a dot surface state. Both types of PL peaks are red shifted relative to the absorption peak.

The redshift of the intrinsic, short-lifetime global PL peak is quite large,[16,17] being 180 meV for an average size of 30 Å. As shown schematically in Fig. 1~c!, this nonresonant redshift arises because one excites *more than one* inhomogeneously broadened electronic state ~e.g., $E^{(1)}_{\rm fast}$ and $E^{(2)}_{\rm fast}$! as compared to a single inhomogeneously broadened state in selective excitation @Fig. 1~d!#.

The redshift of the long-lifetime PL peak could be due to surface defect for three reasons. ~a! The peak is removed by HF surface etching. ~b! The long-lifetime PL peak is measured[16] ; 350 meV below the dot-interior related PL peak for the dot with d ' 30 Å. Our calculation shows that for dot sizes less than 57 Å, the In DB state is below the dot-interior CBM state ~Fig. 8!. For the $d=26$ Å dot, the In DB surface state is predicted to lie 300 meV below the dot-interior CBM state, in good agreement with the experimental value. ~c! The measured ratio[16] of the lifetime of the surface-related PL peak to that of the dot-interior peak is 10–100 for d ' 30 Å. Our calculation ~Table II! for the nearest size $d=26$ Å shows that the lifetime ratio of the VBM to In DB transition to the VBM to CBM transition is 18. Our calculation also shows that this lifetime ratio increases with increasing dot size.

The results of Fig. 8 and Table II then suggest that the In DB state is a possible origin of the low-energy, slowly emitting state $\Vdash E_{\rm slow}\&$ ~Fig. 2! observed[16] in global excitation @Fig. 1~c!# prior to HF etching of the dot. The strong absorption will occur from the VBM to the CBM, following an intersystem crossing to the In DB state, which is the slowly emitting state for dots smaller than 57 Å. The surface-state-induced redshift will vanish for dots larger than 57 Å, where the lowest unoccupied state becomes the dot-interior CBM state. The redshift $E_{\rm CBM}-E_{\rm In\,DB}$ is plotted in Fig. 5 with respect to the excitonic gap ~which is close to $E_{\rm CBM}-E_{\rm VBM}$!, showing a nearly linear dependence.[66]

Bawendi and co-workers[11] found that the red-shifted FLN emission spectrum of CdSe dots closely resembles the absorption spectrum ~as measured by pump-probe experiment!. Since in a surface state model the absorption and emission will presumably commence from spatially *different* electronic states ~''corelike'' and ''surfacelike''!, the spectral resemblance of absorption and emission suggested to them that some intrinsic states are involved rather than surface states. This is not a compelling argument since the surface dangling-bond state and the dot-interior conduction state are electronically coupled so their spectral properties could very well resemble each other.

2. Selective excitation experiments and the singlet-triplet states

While the 350-meV redshift observed in *global excitation experiments*[16] prior to etching can be tentatively explained by the surface-defect mechanism, as we will see below, the redshift seen in *selective excitation* @Fig. 1~d!# for HF-etched and passivated InP dots[17] cannot. Before comparing theory and experiment, however, we need to analyze the experimental FLN data[17] to extract from it the quantity that is comparable with theory. Conventional samples include dots of many sizes $\$d\%$, with a typical size distribution[67]

$$P\sim d,\wedge d\&!=\frac{1}{\sqrt{2\pi}\,s_d}\,e^{-\sim d-\wedge d\&!^2/2s_d^2}, \qquad \sim 6!$$

with the average size $\wedge d\&$. The standard deviation s_d can be deduced from transmission electron microscopy ~TEM!.[16] Because of the existence of a size distribution of dots, each emitting at its own characteristic energy, the measured emission line shape represents an ensemble average, denoted here as $\overline{I_{\rm PL}}(\ll,\ll_{\rm excit},\wedge d\&)$, where $\ll_{\rm excit}$ is the excitation energy. It is of interest to extract from the measured $\overline{I_{\rm PL}}(\ll,\ll_{\rm excit},\wedge d\&)$ versus $\ll_{\rm excit}$ the underlying single-dot redshift for two reasons: ~i! Theory calculates single-dot quantities, not the ensemble average, and ~ii! part of the observed ensemble redshift is due to the size distribution effect, not an intrinsic effect, and it is necessary to separate these contributions.

To extract the single-dot redshift from the measured FLN, we simulate the ensemble emission intensity as

$$\overline{I_{\rm PL}}\sim\ll,\ll_{\rm excit},\wedge d\&!=\int_{d>d_c\sim\ll_{\rm excit}!} a\sim\ll_{\rm excit},d!I_{\rm PL}\sim\ll,d!P\sim d,\wedge d\&!. \qquad \sim 7!$$

Here $a(\ll_{\rm excit},d)$ is the single-dot absorption coefficient at the energy $\ll_{\rm excit}$ and $I_{\rm PL}(\ll,d)$ is the single-dot emission intensity. We assume that each dot absorbs at the energy $\ll_{\rm excit}>E$

where B and m are to be determined by fitting the measurements. The sum over d in Eq. ~7! is limited to those values satisfying $E_g(d) < \hbar\omega_{\mathrm{excit}}$.

We fitted the data of Micic *et al.*[17] for $\langle d \rangle = 32$ Å, using $\sigma_d = 2.5$ Å ~the average of the TEM measured values of Ref. 16! and $\sigma_{\mathrm{PL}} = 2$ meV and taking $a(\omega, d)$ to be a constant over the small range of excitation energies involved. Denoting the energy of the peak of the ensemble emission $I_{\mathrm{PL}}(\omega, \omega_{\mathrm{excit}}, \langle d \rangle)$ as $\omega_{\mathrm{peak}}(\omega_{\mathrm{excit}}, \langle d \rangle)$, we define the ensemble redshift as

$$\tilde{D}(\omega_{\mathrm{excit}}, \langle d \rangle) \equiv \omega_{\mathrm{excit}} - \omega_{\mathrm{peak}}(\omega_{\mathrm{excit}}, \langle d \rangle). \quad (11)$$

Here only the main conclusions about the single-dot redshift are discussed, while the detail of the simulation results

decreases as the dot becomes larger. The In DB state is related, most likely, to the redshifted emission observed at 1.46 eV of the unetched InP dots and is responsible for the low quantum emission efficiency. Such surface defect states are predicted to show *large* redshifts (; 500 meV) with a size-dependent ~long! radiative lifetime.

~vi! Removal of an anion-passivating atom results in a P dangling-bond state that lies above the intrinsic dot valence band for all dot sizes and has a very weak dipolar coupling to the conduction band. This state is strongly localized and would act as an effective ~lifetime shortening! trap for photogenerated holes. This state interacts strongly with the dot intrinsic VBM, shifting it to higher energies ~by up to 250 meV! relative to fully passivated dots.

~vii! An analysis of the *sample-averaged* resonant redshift $\tilde{D}(\hbar\omega_{excit})$ observed in selective excitation experiments reveals that it is considerably larger than the inferred *single-dot* redshift $D(\hbar\omega_{excit})$ from which size-distribution effects have been deconvoluted.

~viii! The calculated In dangling-bond state induces a redshift that is too large to explain the observed resonant, single-dot redshift (<20 meV). It is not impossible that more complex surface chemistry could, however, explain this shift.

~ix! The calculated single-triplet exchange splittings for a *screened* exchange interaction agree well with the observed resonant single-dot redshift. This type of redshift is predicted to be small (<20 meV) and the redshifted emission has but a weak size dependence of its ~long! radiative lifetime.

The effect of vibronic coupling, leading possibly to a change in the equilibrium geometry of the electronically excited dot ~and thus to a Frank-Condon-type redshift!, was not considered here.

ACKNOWLEDGMENTS

We thank A. Franceschetti, L. W. Wang, and S. B. Zhang for helpful discussions on the theory and O. I. Micic and A. J. Nozik for helpful discussions on their data. This work was supported by the U.S. Department of Energy, OER-BES, under Grant No. DE-AC36-83CH10093.

[1] P. D. J. Calcott, K. J. Nash, L. T. Canham, M. J. Kane, and D. Brumhead, J. Phys. C **5**, L91 ~1993!.

[2] V. Petrova-Koch, T. Muschik, A. Kux, B. K. Meyer, F. Koch, and V. Lehmann, Appl. Phys. Lett. **61**, 943 ~1992!.

[3] F. Koch, V. Petrova-Koch, T. Muschik, A. Kux, F. Muller, V. Garilenko, and F. Moller, in *Proceedings of the 21st International Conference on the Physics of Semiconductors, Beijing, 1993*, edited by H. Z. Zheng and P. Jiang ~World Scientific, Singapore, 1993!, p. 1483.

[4] F. Koch, V. Petrova-Koch, T. Muschik, A. Kux, F. Muller, and V. Garilenko, in *Microcrystalline Semiconductors: Materials Science & Devices*, edited by P. M. Fauchet *et al.*, MRS Symposia Proceedings No. 283 ~Materials Research Society, Pittsburgh, 1993!, p. 197.

[5] F. Koch, V. Petrova-Koch, and T. Muschik, J. Lumin. **57**, 271 ~1993!.

[6] Y. Kanemitsu, T. Futagi, T. Matsumoto, and H. Mimura, Phys. Rev. B **49**, 14 732 ~1994!.

[7] M. G. Bawendi, W. L. Wilson, L. Rothberg, P. J. Carroll, T. M. Jedju, M. L. Steigerwald, and L. E. Brus, Phys. Rev. Lett. **65**, 1623 ~1990!.

[8] M. G. Bawendi, P. J. Caroll, W. L. Wilson, and L. E. Brus, J. Chem. Phys. **96**, 946 ~1992!.

[9] D. J. Norris, A. Sacra, C. B. Murray, and M. G. Bawendi, Phys. Rev. Lett. **72**, 2612 ~1994!.

[10] M. Nirmal, C. B. Murray, and M. G. Bawendi, Phys. Rev. B **50**, 2293 ~1994!.

[11] D. J. Norris and M. G. Bawendi, J. Chem. Phys. **103**, 5260 ~1995!.

[12] M. Nirmal, D. J. Norris, M. Kuno, M. G. Bawendi, Al. L. Efros, and M. Rosen, Phys. Rev. Lett. **75**, 3728 ~1995!.

[13] Al. L. Efros, M. Rosen, M. Kuno, M. Nirmal, D. J. Norris, and M. Bawendi, Phys. Rev. B **54**, 4843 ~1996!.

[14] M. O'Neil, J. Marohn, and G. Mclendon, J. Phys. Chem. **94**, 4356 ~1990!.

[15] A. Hasselbarth, A. Eychmuller, and W. Weller, Chem. Phys. Lett. **203**, 271 ~1993!.

[16] O. I. Micic, J. Sprague, Z. Lu, and A. J. Nozik, Appl. Phys. Lett. **68**, 3150 ~1996!; O. I. Micic, C. J. Curtis, K. M. Jones, J. R. Sprague, and A. J. Nozik, J. Phys. Chem. **98**, 4966 ~1994!; O. I. Micic ~private communication!.

[17] O. I. Micic, M. Cheong, J. Sprague, A. Mascarenhas, H. Fu, A. Zunger, and A. J. Nozik, J. Phys. Chem. ~to be published!.

[18] S. Fafard, D. Leonard, J. L. Merz, and P. M. Petroff, Appl. Phys. Lett. **65**, 1388 ~1994!.

[19] M. Grundmann, J. Christen, N. N. Ledentsov, J. Bohrer, D. Bimberg, S. S. Ruvimov, P. Werner, U. Richter, J. Heydenreich, V. M. Ustinov, A. Yu. Egorov, A. E. Zhukov, P. S. Kopev, and Zh. I. Alferov, Phys. Rev. Lett. **74**, 4043 ~1995!.

[20] T. Takagahara, Phys. Rev. B **47**, 4569 ~1993!; T. Takagahara and K. Takeda, *ibid.* **53**, R4205 ~1996!.

[21] U. Woggon, F. Gindele, O. Wind, and C. Klingshirn, Phys. Rev. B **54**, 1506 ~1996!.

[22] G. L. Bir and G. E. Pikus, *Symmetry and Strain-Induced Effects in Semiconductors* ~Wiley, New York, 1975!, p. 285.

[23] E. Martin, C. Delerue, G. Allan, and M. Lannoo, Phys. Rev. B **50**, 18 258 ~1994!.

[24] A. Franceschetti and A. Zunger, Phys. Rev. Lett. **78**, 915 ~1997!.

[25] T. Richard, P. Lefebvre, H. Mathieu, and J. Allegre, Phys. Rev. B **53**, 7287 ~1996!.

[26] A. Franceschetti and A. Zunger, Phys. Rev. B **52**, 14 664 ~1995!; Appl. Phys. Lett. **68**, 3455 ~1996!.

[27] G. B. Grigoryan, E. M. Kazaryan, Al. L. Efros, and T. V. Yazeva, Fiz. Tverd. Tela ~Leningrad! **32**, 1772 ~1990! @Sov. Phys. Solid State **32**, 1031 ~1990!#.

[28] L. W. Wang and A. Zunger, J. Phys. Chem. **98**, 2158 ~1994!; J. Chem. Phys. **100**, 2394 ~1994!.

[29] C. Y. Yeh, S. B. Zhang, and A. Zunger, Phys. Rev. B **50**, 14 405 ~1994!.

[30] C. Delerue, M. Lannoo, and G. Allan, J. Lumin. **57**, 249 ~1993!.

[31] G. Allan, C. Delerue, and M. Lannoo, Phys. Rev. Lett. **76**, 2961 ~1996!.
[32] M. A. Tischler, R. T. Collins, J. H. Stathis, and J. C. Tsang, Appl. Phys. Lett. **60**, 639 ~1992!.
[33] M. S. Brandt and M. Stutzmann, Appl. Phys. Lett. **62**, 2569 ~1992!.
[34] J. R. Sachleben, E. W. Wooten, L. Emsley, A. Pines, V. L. Colvin, and A. P. Alivisatos, Chem. Phys. Lett. **198**, 431 ~1992!.
[35] L. Becerra, C. B. Murray, R. G. Griffin, and M. G. Bawendi, J. Chem. Phys. **100**, 3297 ~1994!.
[36] J. E. Bowen Katari, V. L. Colvin, and A. P. Alivisatos, J. Phys. Chem. **98**, 4109 ~1994!.
[37] S. A. Majetich, A. C. Carter, J. Belot, and R. D. McCullough, J. Phys. Chem. **98**, 13 705 ~1994!.
[38] G. Allan, C. Delerue, and M. Lannoo, Phys. Rev. B **48**, 7951 ~1993!.
[39] Al. L. Efros, Phys. Rev. B **46**, 7448 ~1992!; Al. L. Efros and A. V. Rodina, *ibid.* **47**, 10 005 ~1993!.
[40] S. Nomura, Y. Segawa, and T. Kobayashi, Phys. Rev. B **49**, 13 571 ~